Theor Chem Acc (1999) 101:234–240
DOI 10.1007/s00214980m116

Theoretical
Chemistry Accounts

Regular article

Transition-state structures for describing the enzyme-catalyzed mechanisms of rubisco*

J. Andrés[1], **M. Oliva**[1], **V. S. Safont**[1], **V. Moliner**[1], **O. Tapia**[2]

[1] Departament de Ciències Experimentals, Universitat Jaume I, P.O. Box 224, E-12080 Castelló, Spain
[2] Department of Physical Chemistry, Uppsala University, P.O. Box 532, S-75121 Uppsala, Sweden

Received: 24 March 1998 / Accepted: 3 September 1998 / Published online: 10 December 1998

Abstract. The carboxylation and oxygenation processes of a model substrate, 3,4-dihydroxy-2-pentanone, have been theoreticaly characterized as a set of steps, mimicking the corresponding reactions of D-ribulose-1,5-bisphosphate catalyzed by rubisco. A theoretical characterization is carried out of transition-state structures and possible molecular intermediates represented as saddle points of index 1 and minimum energy structures, respectively. The quantum chemical characterization, at the HF/3-21G calculation level, of these stationary points is used to rationalize and to discuss both catalyzed sequences. The reported set of these stationary points maps out most experimental aspects of the reaction pathways for the real system.

Key words: Rubisco mechanism – Transition-state structures – Ab initio calculations

1 Introduction

Saddle points of index 1 [1, 2], referred to as transition-state structures (TSSs), are reported for a five-carbon model of D-ribulose-1,5-bisphosphate (RuBP) submitted to carbon dioxide and oxygen attack at the C2 center. They map the carboxylation and oxygenation mechanisms of rubisco-catalyzed reactions. This study is made for the model system in vacuum. At first sight, there is a lack of groups in the environment which may be responsible for catalytic activity and efficiency. It is then clear, from the start, that the type of study reported here addresses a more fundamental issue: whether or not minimal molecular models exist that can sustain all the chemistry without any assistance from the environment. If these exist, then a comparison with experimentally determined TS analogs can be used to accept or discard them. If the geometry (and consequently the molecular surface) are superposable, then they can be seen as candidates to mediate the actual reaction, as surface complementarity with the active site would satisfy Pauling's criterion for enzyme catalysis: otherwise, they are simply irrelevant. The import of functional groups would come in the discussion at this stage since docking of the theoretical structures into the real enzyme may offer an alternative way to discuss catalysis. A next step in this type of approach is to increase the size of the models, so that more and more groups which appear to be important from the X-ray structure are taken into account. As we show in a companion paper, checking whether or not saddle-point nature is conserved or drastically changed yields a fundamentally new piece of theoretical information. The present study shows that the reactions may be carried out with minimal motion of the substrate with a model not requiring protein groups.

From the mechanistic point of view, rubisco is a complex system. Besides bi-functionality, namely oxygenation and carboxylation which are chemical steps which happen at the same active site and which operate on the same carbon center (C2) of RuBP [3–6], the system may be self-inhibited by isomerization in situ of RuBP [7–9]. Moreover, in the carboxylation path there is a configuration inversion at C2 following the C2—C3 bond-breaking process. The presence of an intermediate dienol opening the reactive path is an important element in the experimental description of the overall reactivity [3–6, 10, 11]. Gem-diol and aci-acid intermediates have also been suggested to explain the kinetics of this system. In this paper we show that a thorough characterization of TSSs can be used to give a reasonable electronic description for both molecular mechanisms.

The mechanistic picture obtained from the TSSs corresponds with the experimentally available information in spite of the fact that such structures are determined in vacuum. As noted by us earlier [12–14], TSSs for carbon dioxide and oxygen attack can be overlayed on the geometric structure of the TS analog CABP

*Contribution to the Proceedings of Computational Chemistry and the Living World, April 20–24, 1998, Chambery, France

Correspondence to: J. Andrés

(2-carboxyarabinitol bisphosphate) that was obtained from high-resolution X-ray spectroscopy by Andersson [15]. This fact suggests that the enzyme would present a molecular surface that is complementary in shape to the activated complexes of both reactions if the calculated geometries are not too different from this analog. The discussion of mechanistic issues is then based upon Pauling's lemma [16–18]. The present work describes all aspects related to the elementary steps in the oxygenation and carboxylation mechanisms.

2 Rubisco

RuBp carboxylase/oxygenase (rubisco, E.C.4.1.1.39) catalyzes the initial step in Calvin's reductive pentose phosphate cycle, i.e. the photosynthetic fixation of atmospheric carbon dioxide to the enzyme's substrate RuBP. The enzyme also catalyzes a competing oxygenase reaction, thereby reducing the net efficiency of photosynthesis by up to 50% depending upon the relative concentration of carbon dioxide and oxygen [4, 19–27]. The turnover of 3 s^{-1} reflects an inefficient enzyme. This inefficiency is overcome by the abundancy of the enzyme which ensures an annual fixation of 10^{11} tons of carbon dioxide from the atmosphere to the biosphere. An improvement of the biomass production would require the photorespiration reaction to be repressed. For this reason, genetic redesign of rubisco aimed at increasing the discrimination power between carbon dioxide and oxygen is still attracting much interest. Unfortunately, all efforts made to date in this direction have been unsuccessful: either the mutant proteins did not catalyze the addition of gaseous species [28], or the discrimination against oxygen even declined with respect to the in vivo value [29–32].

From the carboxylation process of RuBP to the production of two molecules of 3-phospho-D-glycerate (PGA), the catalytic reaction involves different steps, some of which can occur as partial reactions forming intermediates [33]. Oxygenation starts from the same carbon frame derived from carboxylation by producing a hydroxyperoxide structure, followed by hydration and gem-diol formation at C3 and ending with the step associated with an intramolecular deprotonation process with concomitant scissions of the C2—C3 and O—O bonds with formation of PGA and 2-phosphoglycolate molecules. The commonly accepted reaction steps are depicted in Fig. 1 for carboxylation and oxygenation of RuBP [3, 4]. Enolization is the first and possibly rate-limiting step [15, 34–40]. The overall carboxylation and oxygenation reactions can be dissected into a series of consecutive steps: carbon dioxide or oxygen fixation, hydration, C2—C3 bond breaking and an additional inversion of configuration at the C2 center for the carboxylation sequence [3, 4, 41].

3 Model system and computing methods

2-Keto-3,4-dihydroxypentane is used as a model system of the substrate RuBP. Compared to the real substrate, only the two phosphates attached to carbon atoms 1 and 5 are not present. The phosphate groups contribute to

Fig. 1. Schematic reaction pathway for the carboxylation and oxygenation of D-ribulose-1,5-bisphosphate *RuBP* catalyzed by rubisco extracted and modified from Ref. [4]

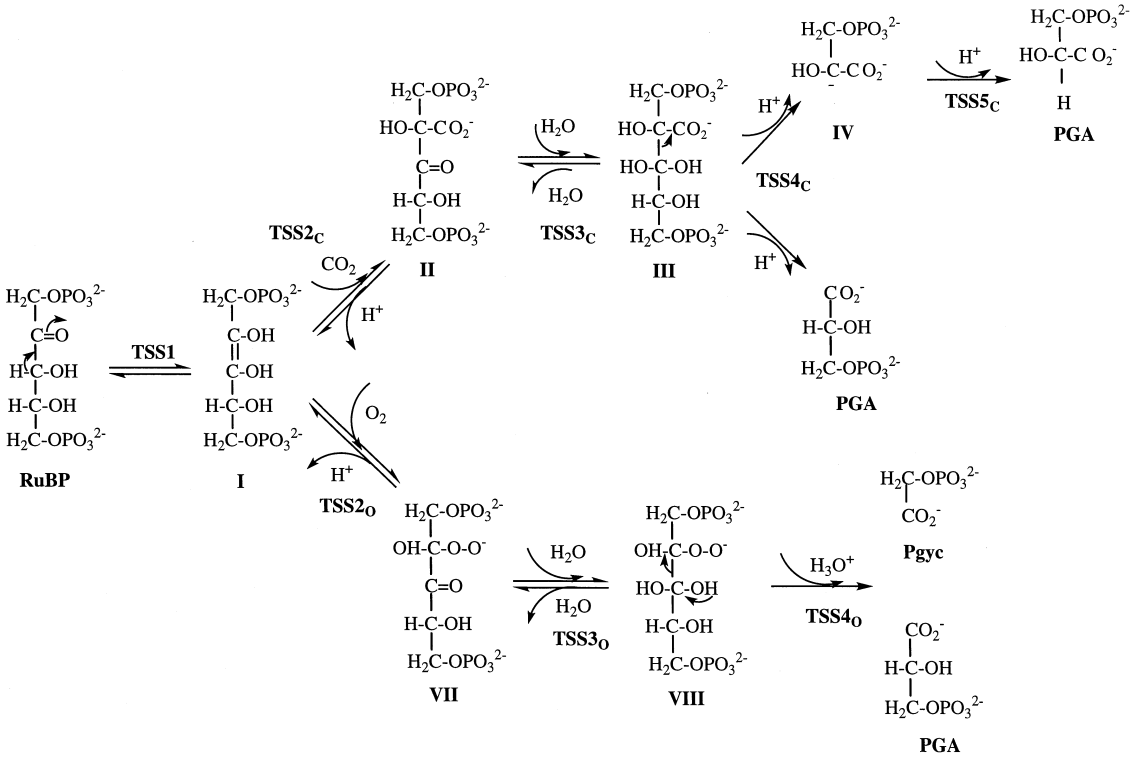

a productive binding as documented experimentally by X-ray studies [3, 4, 15, 42–44]. Besides, these X-ray data had systematically excluded the participation of residues acting as acid/base groups due to the large distance to the substrate's atoms to be protonated-desprotonated [15, 44] except for the carbamylated Lys 201 and His 294 (Spinach numbering). Therefore, a model system without inclusion of external groups has been used by us [10].

The stationary points were located by optimizing the geometries at the HF/3-21G basis set level, because previously we have found similar results with different levels of computing, such as semiempirical AM1 [9], HF/4-31G [10], HF/6-31G** [45], MP2/6-31G**, or even QM/MM methods [46]. Berny analytical gradient optimization routines were used [47, 48]. The density matrix converged to within 10^{-9} a.u.; the threshold values of maximum displacement and maximum force were 0.0018 Å and 0.00045 hartree/bohr, respectively. The nature of each stationary point was established by calculating and diagonalizing the Hessian matrix (force constant matrix). The intrinsic reaction coordinate (IRC) [49] path was traced in order to check the energy profiles connecting each TS to the associated minima of the proposed mechanism by using the second-order González-Schlegel integration method [50, 51]. All calculations were carried out using the GAUSSIAN 94 program [52]. Supplementary vibrational and spectral analysis was made with the AMPAC 5.0 package [53].

The strategy followed for obtaining the TS starts by searching for it in the quadratic zone on the energy hypersurface. The exact characterization of the saddle point of index 1 structures is achieved by using a simple algorithm [10, 54, 55] in which the coordinates describing the system are separated into two sets: the control space, which is responsible for the unique negative eigenvalue in the respective force constant matrix [56], and the remaining coordinates referred to as complementary space. The geometry optimizations are carried out alternatively on each subspace, one at a time, until the stationary structure is obtained. Finally, a complete analytical optimization was achieved for the complete space of all variables. Examination of the TSSs is achieved by the evaluation of the Hessian matrix; the nature of these stationary points was established by calculating analytically and diagonalizing this matrix of energy second derivatives to determine the unique imaginary frequency. Once the stationary points are obtained, the Hessian is recalculated and the transition vector, which yields, at zero order, very concisely the essentials of the chemical process under study [56, 57]. A calculation of normal modes is carried out.

4 Carboxylation and oxygenation pathways

An overview of these pathways, as obtained from the calculations of stationary points, is presented in Fig. 2. Once the enzyme is activated, enolization is generally accepted as the first and rate-limiting step in the molecular mechanism of rubisco [15, 34–40]. For this tautomerization process we have characterized a TSS1 (cf. Fig. 3) associated with the intramolecular proton transfer from the C3 hydroxyl to the ketone group linked to the C2 center. The 2,3-enediol formed here is the reactant fragment for carboxylation and the competing oxygenation; in both reactions, the C2 center is attacked. A close look at Fig. 2 shows a number of similarities in the first stages of both mechanisms that are now discussed.

First, they share the enolization transition structure TSS1. This is depicted in Fig. 3. The geometry of this species is very different from the ground-state minimum energy structure of the reactant (see Fig. 2), although it resembles the enediol structure and the carbon framework of the remaining stationary points reported here. The transition vector involves five atoms. In order to get at it, the carbon framework must be severely torsioned around the C2—C3 bond axis if one uses the structure of minimum energy (RuBP model). This feature coincides with the deformed carbon frame of CABP [15]. The remarkable fact is that TSS1 is a stationary structure in vacuum. As this TSS has already been discussed by us [10, 11] we can turn now to the next specific step.

The attack of carbon dioxide or oxygen is made on the same C2 position. One obtains $TSS2_C$ and $TSS2_O$ shown in Figs. 4 and 5, respectively. The carbon frames are very similar in space orientation. Small differences arise that do not change what may be their molecular surface when this is calculated for TSS1 or $TSS2_C$ and $TSS2_O$. This similarity would imply that both processes may take place at the same active site. Another similarity is the proton exchange at the entrance channel from the hydroxyl group at C3 toward the entering attacking molecule. In both cases, a carbonyl group is prompted at C3 and an acid intermediate (A) or a protonated hydroxyperoxide (H) moiety appears as an intermediate. Note that, at variance with the standard mechanism (cf. Fig. 1), by considering the possibility of intramolecular proton transfer, there would be no need for an external base to abstract the hydrogen at C3. Of course, this is not to be taken as a statement denying a role for external groups during actual catalysis. The results point towards a minimal motion alternative only.

As the next step must be hydration at the C3 center, one can see that the corresponding carbonyl group is there to be hydrated in both cases, and $TSS3_C$ and $TSS3_O$ are obtained. The hydration in A leads to $TSS3_C$, a four-membered ring, corresponding to a concerted mechanism such that oxygen addition to C3 and proton transfer to the carbonyl oxygen are accomplished in a single step. This type of transition structure has been found in related hydration of carbonyl compounds [58]. $TSS3_C$ is related by its transition vector with the gem-diol intermediate (G). Experimentally, such a type of functionality has been used in connection with the mechanism of rubisco [4, 59]. The gem-diol has a strong acid character that would facilitate a new intramolecular hydrogen rearrangement. As shown later, the deprotonation of the gem-diol is related to the breaking of the carbon-carbon bond between the C2 and C3 centers.

$TSS3_O$ results, corresponding to the direct hydration of the carbonyl group of H to yield a HH system. The related product (albeit geometrically deformed) is the equivalent of structure VIII in Fig. 1. This time, how-

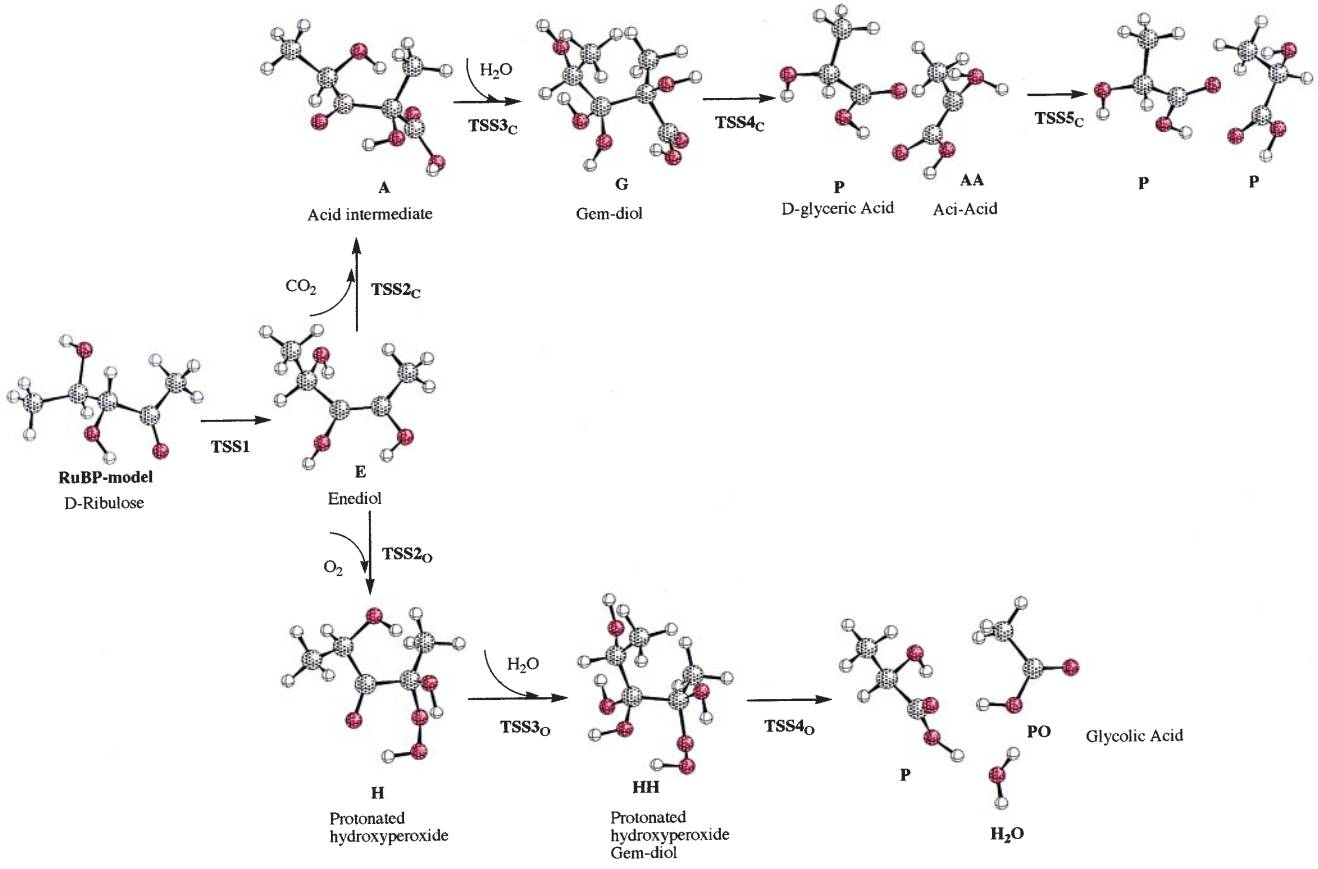

Fig. 2. Schematic reaction pathway for the enolization, carboxylation and oxygenation obtained from ab initio calculations on a five-carbon model (see the text for descriptions). Energies of the stationary points relative to the enediol (kcal/mol) are as follows. Carboxylation process: reactants ($E + H_2O + CO_2$) = 0; $TSS2_C$ ($+H_2O$) = 39.11; A ($+H_2O$) = −18.46; $TSS3_C$ = 21.98; G = −23.37; $TSS4_C$ = 32.75; $P + AA$ = 12.50; $TSS5_C$ = 43.64; $P + P$ = −40.25. Oxygenation process: reactants ($E + H_2O + O_2$) = 0; $TSS2_O$ ($+H_2O$) = 7.71; H ($+H_2O$) = −26.71; $TSS3_O$ = −8.60; HH = −55.49; $TSS4_O$ = 36.18; $P + PO + H_2O$ = −140.37

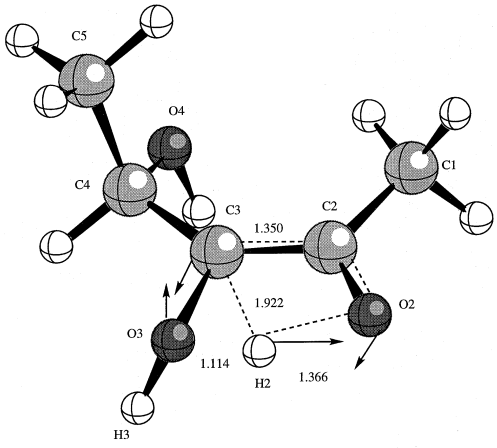

TSS1

Fig. 3. TSS1 for the enolization step obtained from HF/3-21G calculations on a five-carbon model. The *arrows* represent the major components of the corresponding transition vector. The main distances (in angstroms) are also included

ever, the protonated peroxide forms a strong hydrogen bond with the carbonyl oxygen at C3. A new transition structure thereby becomes accessible via intramolecular hydrogen transfer.

It is worth noting that there is no way to differentiate both mechanisms, at least during the first three steps; however, once the system has gone that far (along either path) there is no way to bring it back. All other steps, for the calculated mechanism, can be executed as intramolecular hydrogen transfers.

The theoretical C2—C3 bond breaking process also has some similarities. They can be sensed from $TSS4_C$ and $TSS4_O$ in Figs. 4 and 5. The C2—C3 bond breaks concomitantly with an intramolecular proton-transfer process. From experimental results it is proposed that the following step, associated with a C2—C3 bond-breaking process, is prompted by the elimination of two protons. The carbon-carbon cleavage has been a puzzling feature for a theoretical explanation of the mechanism. In our case, from structure G of the carboxylation sequence, a fourth $TSS4_C$ is related to a carbon-carbon (C2—C3) cleavage coupled to hydrogen transfer from O3 to the OH group located at C2 producing a biprotonated oxygen and reforming a carbonyl center at C3. The transition vector amplitudes of this $TSS4_C$ resemble the transition structure for an intra-

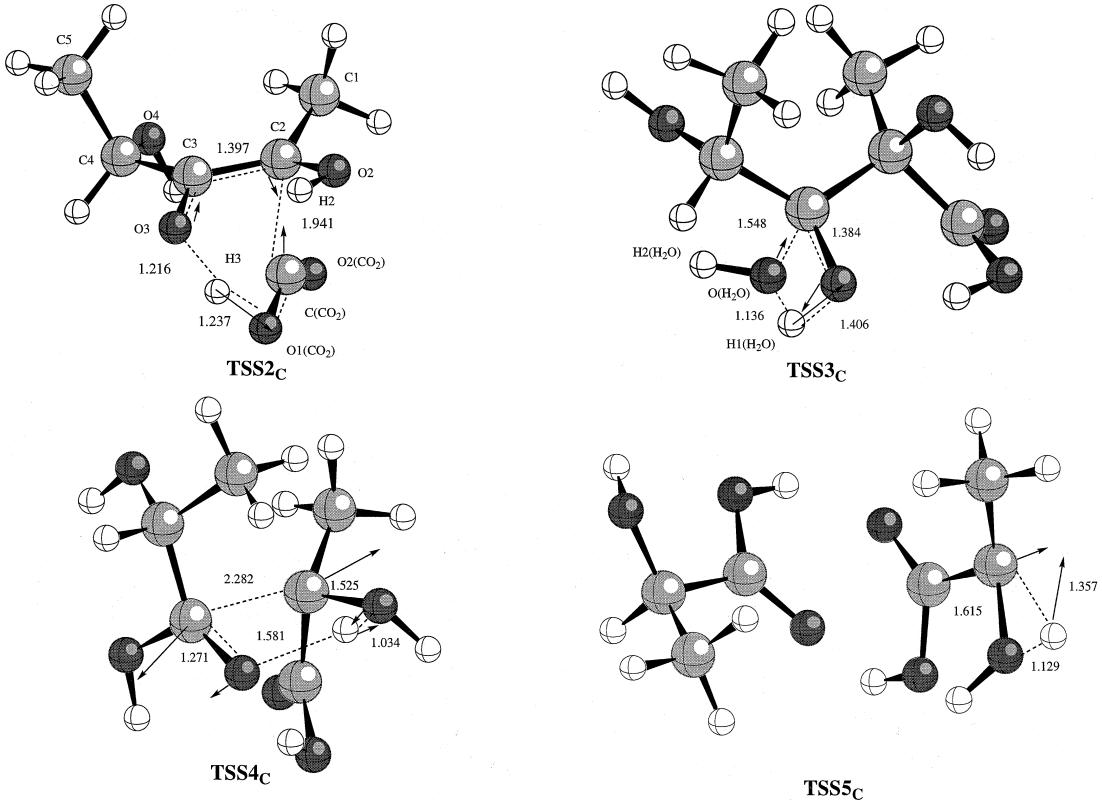

Fig. 4. Transition-state structures for the carboxylation pathway obtained from HF/3-21G calculations on a five-carbon model. The *arrows* represent the major components of the corresponding transition vector

molecular hydrogen-transfer mechanism [9] leading from the substrate-like structure to the dienol structure. Following an IRC procedure, [49] an aci-acid intermediate (AA) and a final D-glyceric acid molecule (P) are formed; P can be related to the PGA product in Fig. 1. The aci-acid AA has a positive charge at the protonated hydroxyl group and a negative charge develops at the adjacent C2 center. Note that this species would prompt an inversion at C2 under specific conditions by 1,2-hydrogen transfer from O2 [45]. For the oxygenation reaction, this is the end of the story. The final transition structure $TSS4_O$ corresponds to simultaneous C2—C3 and $O(O_2)$—$O(O_2)$ bond-breaking processes, and what was the hydrogen of the ingoing water molecule is transferred to the protonated oxygen of the peroxide forming a new water molecule again. The reaction, without hydronium elimination, can simply be accomplished as a complex set of intramolecular processes. Two product molecules form (P and PO) and a water molecule is created at a position corresponding to the magnesium coordination sphere. This latter statement is based on modeling procedures.

For the carboxylation reaction, a final stdep is required to provide an explanation for the most difficult piece of experimental knowledge: the C2 inversion. The AA fragment carrying the carboxylic acid moiety and biprotonated O2 can be submitted to intramolecular hydrogen transfer via $TSS5_C$. There is a hydrogen shift from O2 to C2 with a concomitant inversion of configuration at the C2 center. Note that a similar transition structure could be obtained with no inversion of the configuration. During the bond cleavage step stereospecific protonation and inversion at C2 are required to form a stereochemically correct product. A preliminary study of the carboxylation set of steps modeling the global enzyme structure using hybrid QM/MM methodology indicates that $TSS5_C$ can be docked without steric hindrance into the active center, but the transition structure which would lead to the wrong configuration can not. The present results give a different rationale to Andrews and Lorimer's proposals [3]; the experiments show that there is always inversion of configuration at C2. There is no evidence for the formation of L-PGA by rubisco [60], indicating that this final step is highly specific. The role of an external group from the enzyme is essential to control the direction of the reaction sustained by the minimal model.

5 Discussion

The sequence of TSSs presented in this work shows that, in theory, the system is sufficient to carry out the full reaction if water is available. The reactants molded into geometries characteristic of TSSs occupy the same configurational regions. Of course, this is not to say that the enzyme reaction follows such a pathway without further ado.

The role of the residues making up the coordination shell cannot be assessed from the present vacuum calculations. Modeling suggests that the carbamylated Lys 201 may form a hydrogen bond with the hydroxyl group

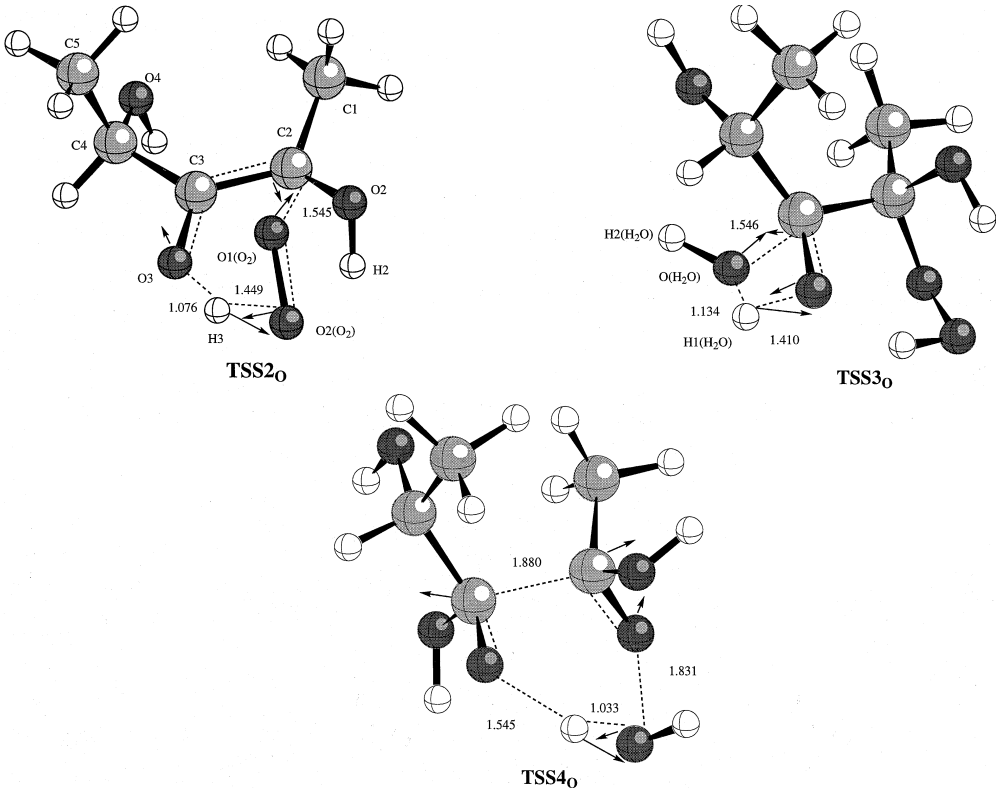

Fig. 5. Transition-state structures for the oxygenation pathway obtained from HF/3-21G calculations on a five-carbon model. The *arrows* represent the major components of the corresponding transition vector

of C2. One should also have a clear understanding of the role played by substrate binding. In particular, Lys 175 is essential for substrate binding and probably may contribute an alternative path for C2 inversion during carboxylation [61]. As indicated by CABP and other crystallographic studies, binding molds the structure into something resembling what will be required to fit in the active site of this enzyme.

The approach described in this and other work is based on the idea that the TSS characterizes a real molecule. It certainly has a finite lifetime. However, if the system is going to take the mechanistic path it should populate the vibrational-librational states obtained for the TSS. The normal mode animations show a number of low-frequency modes localized on the atoms affected by the chemistry. The atom used to bind into the enzyme has very low or zero amplitude. Interconversion takes place as described elsewhere [62].

The structural invariance of the TSS has also been tested using different wavefunctions and molecular models. In a recent work, a three-carbon model presented equivalent TSSs [14, 45] to those reported here. This result is reinforced by our QM/MM study [46] where 3525 atoms were considered classically and 29 atoms plus a water molecule were considered in the quantum subspace. The structure of the saddle point of index 1 is very similar to the one calculated here.

The present work shows that the old inevitability hypothesis of rubisco enzyme [63], namely, carboxylation prompts oxygenation, has an electronic/molecular basis. The TSSs of the initial steps display similar geometric arrangements in the carbon frame of the substrate thereby allowing either reaction. The control of the kinetics is then transferred to the relative concentrations of the oxygen and carbon dioxide substrates. Suppression of one reaction would almost always inhibit the other. Although this is bad news for molecular geneticists, it is good news for people working on theoretical representations of enzyme catalysis. But there is more. In a recent definitive review of experimental information on rubisco, Lorimer and coworkers [63] remarked that 20 years ago, Hanson and Rose [65] suggested that natural selection for catalytic efficiency has led to: (1) the use of the minimum number of acidic and basic groups, (2) the maximum separation of catalytic groups and/or replacing groups, (3) minimal motion of the substrate. It is amazing to see that the set of stationary points calculated here for both reactions complies at least with principles 1 and 3.

Acknowledgements. This work was supported by research funds from the DGICYT (Project PB93-0661 and PB96-0795-C02-02)). Calculations were performed on an IBM RS6000 workstation of the Departament de Ciències Experimentals and on two Silicon Graphics Power Challenger L of the Servei d'Informàtica of the Universitat Jaume I. We are indebted to these centers for providing us with computer capabilities. M.O. thanks the Ministerio de Educación y Ciencia for a FPI fellowship. O.T. thanks NFR for financial support.

References

1. Mezey PG (1980) Theor Chim Acta 54: 95
2. Mezey PG (1987) Potential energy hypersurfaces. Elsevier, Amsterdam

3. Andrews TJ, Lorimer GH (1987) In: Hatch MD, Boardman NK (eds) The biochemistry of plants. Academic Press, New York, pp 131–218
4. Hartman FC, Harpel MR (1994) Annu Rev Biochem 63: 197
5. Bowes G, Ogren WL, Hagerman RH (1971) Biochem Biophys Res Commun 45: 716
6. Andrews TJ, Lorimer GH, Tolbert NE (1973) Biochemistry 12: 11
7. Edmonson DL, Badger MR, Andrews TJ (1990) Plant Physiol 93: 1390
8. Edmonson DL, Badger MR, Andrews TJ (1990) Plant Physiol 93: 1376
9. Tapia O, Andres J, Safont VS (1996) J Phys Chem 100: 8543
10. Tapia O, Andres J, Safont VS (1994) J Phys Chem 98: 4821
11. Andres J, Safont VS, Queralt J, Tapia O (1993) J Phys Chem 97: 7888
12. Tapia O, Andres J (1992) Mol Eng 2: 37
13. Tapia O, Andres J, Safont VS (1995) J Mol Struct THEOCHEM 342: 131
14. Oliva M, Safont VS, Andrés J, Tapia O (1998) Chem Phys Lett 294: 87
15. Andersson I (1996) J Mol Biol 259: 160
16. Pauling L (1946) Chem Eng News 24: 1375
17. Pauling L (1948) Nature (Lond) 161: 707
18. Pauling L (1948) Am Sci 36: 51
19. Schneider G, Lindqvist Y, Brändén C-I (1992) Annu Rev Biophys Biomol Struct 21: 119
20. Andrews TJ, Hatch MD (1969) Biochem J 114: 117
21. Laing WA, Christeller JT (1976) Biochem J 159: 563
22. McCurry SD, Pierce J, Tolbert NE, Orme-Johnson WH (1981) J Biol Chem 249: 6623
23. Mott KA, Berry JA (1986) Plant Physiol 82: 77
24. Robinson SP, Portis AR Jr (1989) Plant Physiol 90: 968
25. Sicher RC, Hatch AL, Stumpf DK, Jensen RG (1981) Plant Physiol 68: 252
26. Yokota A, Kitaoka S (1989) Plant Cell Physiol 30: 183
27. Lee EH, Harpel MR, Chen Y-R, Hartman FC (1993) J Biol Chem 268: 26583
28. Hartman FC, Lee EH (1989) J Biol Chem 246: 11784
29. Robinson PD, Martin MN, Tabita RF (1979) Biochemistry 18: 4453
30. Christeller JT, Laing WA (1979) Biochem J 183: 747
31. Jordan DB, Ogren WL (1983) Arch Biochem Biophys 227: 425
32. Chen Z, Yu W, Lee J-H, Diao R, Spreitzer RJ (1991) Biochemistry 30: 8846
33. Lorimer GH, Gutteridge S, Madden MW (1987) In: von Wettstein, D. Chua NH (eds) Plant Molecular Biology. Plenum Press, New York, pp 21–31
34. Saver BG, Knowles JR (1982) Biochemistry 21: 5398
35. Sue JM, Knowles JR (1982) Biochemistry 21: 5404
36. Hartman FC, Soper TS, Niyogi SK, Mural RJ, Foote RS, Mitra S, Lee EH, Machanoff R, Larimer WF (1987) J Biol Chem 262: 3496
37. Lorimer GH, Hartman FC (1988) J Biol Chem 263: 6488
38. Smith HB, Larimer FW, Hartman FC (1988) Biochem Biophys Res Commun 152: 579
39. Schloss JV (1990) In: Aresta M, Schloss JV (eds) Enzymatic and model carboxylation and reduction reactions for carbon dioxide utilization. Kluwer, Dordrecht, pp 321–345
40. Newman J, Gutteridge S (1993) J Biol Chem 268: 25876
41. Hartman FC (1992) In: Plant Protein Engineering. Cambridge University Press, Cambridge, pp 61–92
42. Knight S, Andersson I, Brändén C-I (1990) J Mol Biol 215: 113
43. Gutteridge S, Rhoades D, Herrmann (1993) J Biol Chem 268: 7818
44. Andersson I, Knight S, Schneider G, Lindqvist Y, Lundqvist T, Brändén C-I, Lorimer GH (1989) Nature (Lond) 337: 229
45. Safont VS, Oliva M, Andres J, Tapia O (1997) Chem Phys Lett 278: 291
46. Moliner V, Andrés J, Oliva M, Safont VS, Tapia O (1998) Theor Chem Acc (This issue)
47. Schlegel HB (1982) J Chem Phys 77: 3676
48. Schlegel HB (1982) J Comput Chem 3: 214
49. Fukui K (1970) J Phys Chem 74: 4161
50. Gonzalez C, Schlegel HB (1990) J Phys Chem 94: 5523
51. González C, Schlegel HB (1991) J Chem Phys 95: 5853
52. Frisch MJ, Trucks GW, Schlegel HB, Gill PMW, Johnson BG, Robb MA, Cheeseman JR, Keith T, Petersson GA, Montgomery JA, Raghavachari K, Al-Laham MA, Zakrzewski VG, Ortiz JV, Foresman JB, Cioslowski J, Stefanov BB, Nanayakkara A, Challacombe M, Peng CY, Ayala PY, Chen W, Wong MW, Andres JL, Replogle ES, Gomperts R, Martin RL, Fox DJ, Binkley JS, Defrees DJ, Baker J, Stewart JP, Head-Gordon M, Gonzalez C, Pople JA (1995) Gaussian 94. Gaussian, Pittsburgh, Pa
53. AMPAC 5.0 (1994) Semichem 7128 Summit: Shawnee KS 66216
54. Tapia O, Andres J (1984) Chem Phys Lett 109: 471
55. Tapia O, Andres J, Safont VS (1994) J Chem Soc Faraday Trans 90: 2365
56. McIver JW (1974) Acc Chem Res 7: 72
57. McIver Jr. JW, Komornicki A (1972) J Am Chem Soc 94: 2625
58. Spangler D, Williams IH, Maggiora GM (1983) J Comput Chem 4: 524
59. Miziorko HM, Lorimer GH (1983) Annu Rev Biochem 52: 507
60. Andrews TJ, Kane HJ (1991) J Biol Chem 266: 9447
61. Harpel MR, Hartman FC (1996) Biochemistry 35: 13865
62. Tapia O, Andrés J, Stamato FJM (1996) In: Tapia O, Bestián J (eds) Solvent effects and chemical reactivity. Kluwer, Dordrecht, pp 283–361
63. Lorimer GH, Andrews TJ (1973) Nature (Lond) 243: 359
64. Cleland WW, Andrews TJ, Gutteridge S, Hartman FC, Lorimer GH (1998) Chem Rev 98: 549
65. Hanson KR, Rose IA (1975) Acc Chem Res 8: 1